The size of the metal ion controls the structures of coordination polymers of 2,1,3-benzoselenadiazole

Lucia Myongwon Lee,[a] Philip J. W. Elder,[a] Paul A. Dube,[b] John E. Greedan,[a] Hilary A. Jenkins,[a] James F. Britten,[a] and Ignacio Vargas-Baca,*[a]

[a] *Department of Chemistry and Chemical Biology, McMaster University, 1280 Main Street West, Hamilton, Ontario, Canada L8S 4M1. Fax: 905 522 2508; Tel: 905 525 9140 ext. 23497; E-mail: vargas@chemistry.mcmaster.ca*

[b.] *Brockhouse Institute for Materials Research, McMaster University, 1280 Main Street West, Hamilton, Ontario, Canada L8S 4M1.*

Supplementary Information

Experimental

1. Materials and Methods

The compound benzo-2,1,3-selenadiazole was prepared according to the literature procedure[1] by reaction of o-phenylenediamine with selenium dioxide in ethanol. DMSO was dehydrated by filtering through columns of freshly baked alumina (until the residual resonance of H_2O in the ^{1}H NMR spectrum was undetectable) and was stored over activated molecular sieves until used. All other chemicals were used as received from commercial suppliers. IR spectra were recorded on a Nicolet 6700 FT-IR spectrometer with a resolution of 4cm^{-1}. Melting points were measured on a Thomas-Hoover melting point apparatus.

2. Preparation of compounds 5-9.

In a typical experiment, a solution of the benzo-2,1,3-selendiazole (0.1g, 0.5 mmol) in DMSO (0.5 mL) was slowly diffused into a solution of anhydrous MCl_2 (0.5 mmol) in absolute ethanol (0.9 mL). Crystals of the products usually formed over 24 hours and were isolated by vacuum filtration, washed with diethyl ether (5 mL) and dried under nitrogen. The materials obtained in this way were stored and handled under an atmosphere of dry nitrogen. The products are deliquescent, being easily hydrated while exposed to the atmosphere. Multiple attempts to perform combustion analysis of the sampled were thwarted by the sensitivity of the sample. Instead, the purity of the samples -specially those used for magnetic studies- was assessed by comparison of diffraction data from single crystals with those from powders in sealed capillary tubes. Spectroscopic characterization was therefore limited to vibrational spectroscopy. IR (cm^{-1}) **5:** 2595(s), 2414(w), 2334(w), 2154(w), 2017(w), 1895(w), 1820(w), 1718(w), 1613(w), 1449(m), 1370(w), 1303(w), 1228(w), 1128(w), 1010(w), 905(w), 745(m), 557(w); **6:** 2957(s), 2414(w), 1979(w), 1605(w), 1504(m), 1475(w), 1449(m), 1365(w), 993(w), 769(m), 569(w); **7:** 2948(s), 2416(w), 2353(m), 2019(w), 1900(w), 1729(w), 1515(m), 1466(m), 1368(m), 1163(m), 1040(w), 1019(m), 995(m), 767(m), 566(w); **8:** 2089(w), 2892(w), 2338(w), 1732(w), 1516(w), 1464(w), 1398(m), 1360(w), 1165(m), 1040(m), 996(m), 794(m), 719(m), 567(s); **9:** 3077(m), 2994(w), 2914(m), 2367(m), 1730(w), 1517(m) 1473(s) 1437(m), 1361(m), 1238 (w), 1166(m), 1038 (m), 988 (s), 898(m), 801(s), 770(s), 676(w), 570(s).

X-ray Diffraction. Data for all samples were collected on a Bruker SMART APEX II diffractometer with a CCD area detector, using graphite-monochromated Mo -Kα radiation (λ= 0.71073 Å) at 100(2) K. Once the data collection was completed, the structures were solved using the SHELXTL[2] suite of programs and most structures were refined by full-matrix least squares on all F^2 values with the WinGX package. The data was empirically corrected for absorption and other effects using SADAB. Non-hydrogen atoms were refined anisotropically. Hydrogen atoms were placed at idealized locations using appropriate riding models.

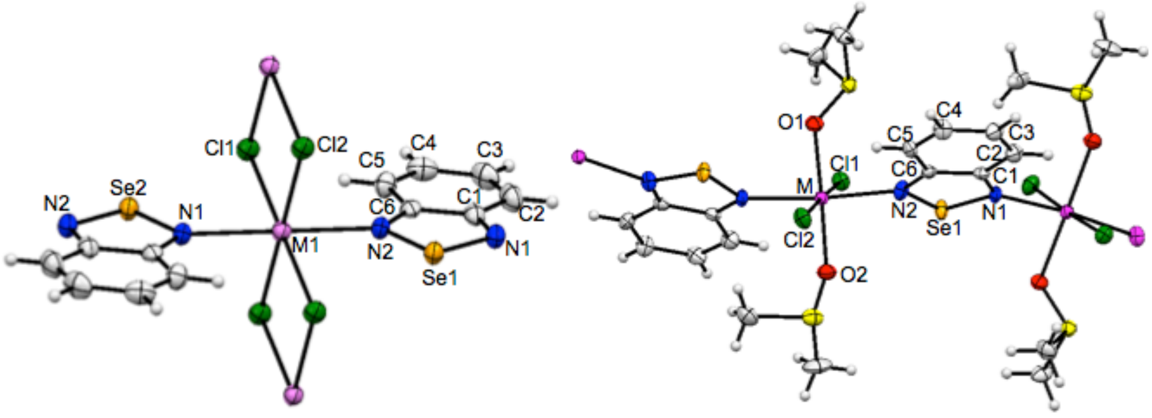

A **B**

Figure S1. Numbering scheme used to report distances and angles in Table 2 for compounds **5,6** (**A**) and **7-9** (**B**).

Magnetic Susceptibility

DC magnetization measurements were performed in a 100 Oe field over the temperature range of 2-300 K using a Quantum Design Magnetic Properties Measurement System with a 5.5 T magnet.

The magnetic parameters and their standard errors were obtained by fitting the nonlinear models to experimental data before antiferromagnetic ordering with Mathematica® 8.0.4.0.

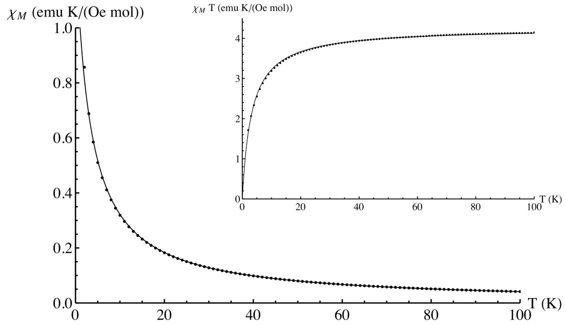

5, M = Mn

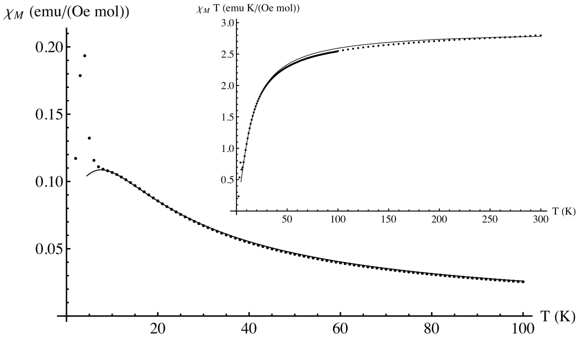

7, M=Fe

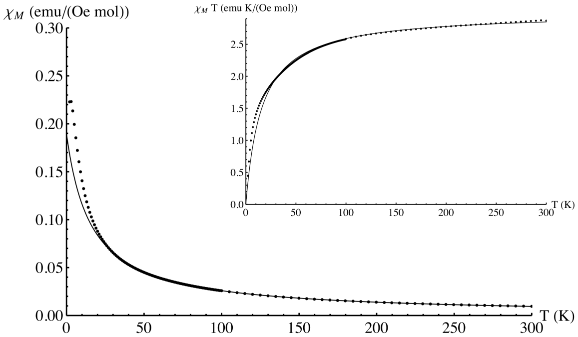

8, M = Co

Figure S2. Temperature dependence of the molar magnetic susceptibilities of **5**, **7** and **8**. Each continuous line is calculated by the corresponding fitted nonlinear model.

Computational Study

The electronic structures of model fragments of the structure were calculated using Hybrid UDFT (ADF,[3] B3LYP[4]/ZORA[5]) from all-electron basis sets basis sets of triple-z quality with two sets of polarization functions. The resulting molecular orbitals were employed in Broken-Symmetry calculations in order to evaluate the *J* coupling constants without spin projection[6] using

$$E_{HS} - E_{BS} = -J(2S_1S_2 + S_2)$$

where E_{HS} and E_{BS} are the high-spin and broken-symmetry energies.

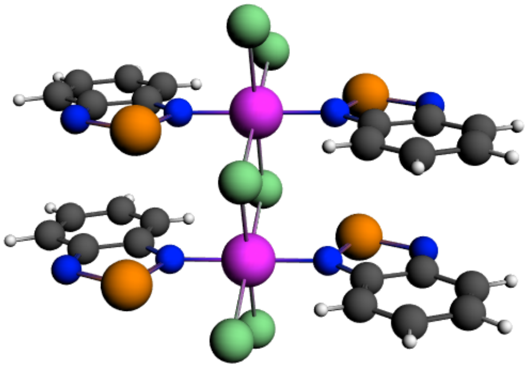

Figure S3. Model used for the calculation of the coupling constant between two Mn^{II} ions along the $[MnCl_2]_\infty$ chains of compound **5** (J = 0.4 K).

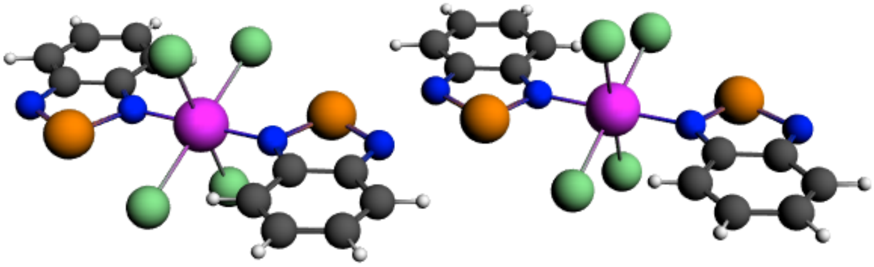

Figure S4. Model used for the calculation of the coupling constant between two Mn^{II} ions through two molecules of benzoselenadiazole and the $[Se\text{-}N]_2$ supramolecular synthon of compound **5** (J = 4,377 K).

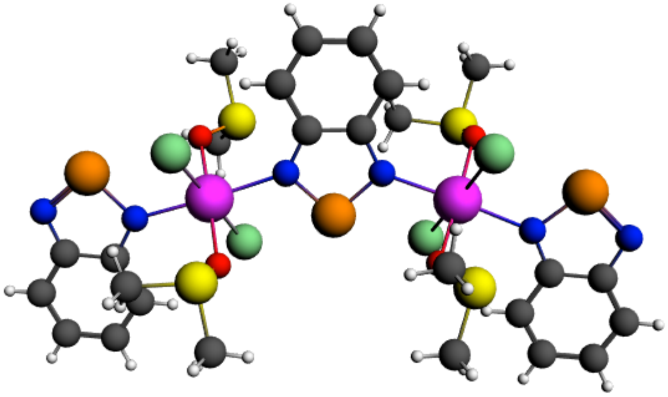

Figure S5. Model used for the calculation of the coupling constant between two M^{II} ions through one molecule of benzoselenadiazole in compounds **7** (M = Fe, J = -216 K), **8** (M = Co, J = 4.2 K), and **9** (M = Ni, 5.6 J = K).

The serious disagreement between the J values calculated in this way and the experimental data indicates that the properties of these materials cannot be accounted from simplistic models for one pair of atoms at a time. In the case of Mn^{II}, the coupling constant along $[MnCl_2]_\infty$ chains is small, as expected from the nearly 90° Cl-Mn-Cl bond angles. The large coupling constant through the ligands (including the $[Se\text{-}N]_2$ supramolecular synthon) suggests that there is spin delocalization on the heterocycles. Calculations for a $[(C_6H_4N_2Se)MnCl_4(C_6H_4N_2Se)]^{2-}$ model afforded a map of spin density (Figure S6) which supports such interpretation. Delocalization of spin into the heterocycle would be enabled by molecular orbitals in the σ and mostly the π frameworks (Figure S7).

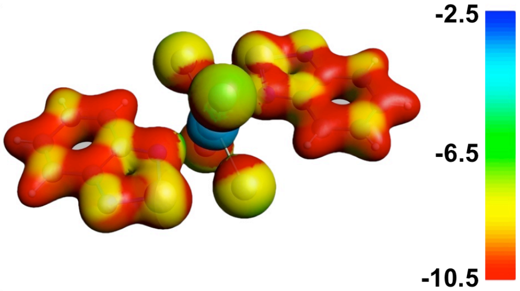

Figure S6. Spin-density (Log_{10} scale of the magnitude in A.U.) of a $[(C_6H_4N_2Se)MnCl_4(C_6H_4N_2Se)]^{2-}$ model projected over the 0.03-A.U electron density isosurface.

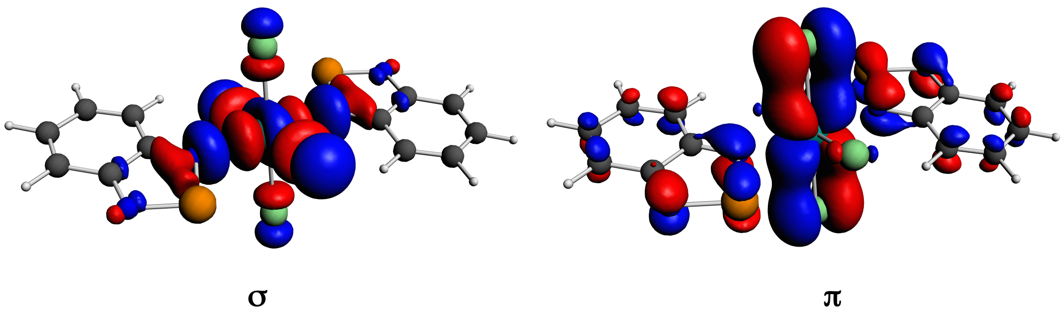
σ
π

Figure S7. Kohn-Sham molecular orbitals that delocalize spin density from the metal ion into the selenadiazole ring of compound **5**.

References

1. Harvey, I.W.; McFarlane, M. D.; Moody, D.J. et al. *J. Chem. Soc. Perkin. Trans,* **1988**, 1939.

2 G. Sheldrick. *Acta Crystallogr. Sect. A*, 2008, **64**, 112-122.

3. a) G. te Velde, F.M. Bickelhaupt, S.J.A. van Gisbergen, C. Fonseca Guerra, E.J. Baerends, J.G. Snijders, T. Ziegler *J. Comp. Chem*. 2001, **22**, 931; b) C. Fonseca Guerra, J.G. Snijders, G. te Velde and E.J. Baerends, *Theor. Chem. Acc*. 1998, **99**, 391; c) ADF2012, SCM, Theoretical Chemistry, Vrije Universiteit, Amsterdam, The Netherlands, http://www.scm.com.

4. a) J. P. Perdew, J. A. Chevary, S. H. Vosko, K. A. Jackson, M. R. Pederson, D. J. Sing and C. Fiolhais, *Phys. Rev. B,* 1992, **46**, 6671; b) P. J. Stephens, F. J. Devlin, C. F. Chabalowski and M. J. Frisch, *J Phys. Chem.* 1994, **98**, 11623.

5. A)E. van Lenthe, A. Ehlers and E. J. Baerends, *J. Chem. Phys*., 1999, **110**, 8943; b) E. van Lenthe, J. G. Snijders and E. J. Baerends, *J. Chem. Phys.,* 1996, **105**, 6505; c) E. van Lenthe, R. van Leeuwen, E. J. Baerends and J. G Snijders, *Int. J. Quant. Chem*., 1996, **57**, 281.
6. A. Rodríguez-Fortea, P. Alemany, S. Alvarez, E. Ruiz, *Chem.–Eur. J.*, **2001**, *7*, 627.